UV LASER ENGRAVING OF HIGH TEMPERATURE POLYMERIC MATERIALS

D. Martinez, L. D. Laude*, K. Kolev and F. Hanus
Université de Mons-Hainaut, 7000 Mons, Belgium
*phone 00 32 65 37 34 20
fax 00 32 65 37 34 27
E-mail: lucien.laude@umh.ac.be

1. INTRODUCTION

Among emerging technologies, those associated with laser sources as surface processing tools are quite promising. In the present work, a UV pulsed (excimer) laser source is experimented for engraving (or ablating) polymeric materials based on three high temperature polymers: polyethylene terephtalate (PET), polyethersulfone (PES) and polyphenylene sulfide (PPS). The ablation phenomenon is demonstrated on all these polymers and evaluated by stylus profilometry upon varying the laser fluence at impact. For each polymer, results give evidence for three characteritic quantities: an ablation threshold E_0, a maximum ablation depth per pulse z_0 and an initial rate of ablation α, just above threshold. A simple ablation model is presented which describes correctly the observed behaviours and associates closely the above quantities to the polymer formulation, thus providing for the first time a rational basis to polymer ablation.The model may be extended to parent plastic materials whenever containing the same polymers. It may also be used to predict the behaviours of other polymers when subjected to excimer laser irradiation.

2. EXPERIMENTAL

Materials

The evaluated sample materials were voluntarily chosen to be all commercially available in order to extrapolate eventual results to specific application domains. Materials are shaped in 1 or 2mm thick molded platelets. The composition of these platelets is shared between the nominal polymer and 30% (massic proportion) glass fiber. The latter consists of 200μm long, 10μm diameter pieces which are gradually distributed from surface to bulk and reach nominal ($\approx$ 10%) volume proportion at some 10μm from surface. The melting temperature of the polymers is 255, 226 and 288°C, for PET, PES and PPS, respectively and their molecular weights are typically large, around 50 000 or more, as usual for commercial products. It is worth to note that the ablation process would only concern the polymer itself, leaving fibers somewhat unaffected even when they would be progressively made accessible to irradiation through the process.

Laser Processing

A (Kr^+F) excimer laser source is used, working at 248 nm (or 5.0eV photon energy) and emitting typically 0.6J (or 6 x 10^{17} of such photons) in 25nsec long pulses at 1sec intervals. The time profile of the light intensity during a pulse is strongly asymetric with 1/e width at 25 nsec, maximum after 5nsec, 40nsec total duration, 50% of the laser energy delivered within the first 10nsec. The beam cross-section is large ($2cm^2$) and homogenized. Upon focusing, that incident laser energy is reduced to an effective density per pulse or fluence ε (in J/cm^2) upon impacting the sample surface. Fluence and number of pulses can be varied in order to provide a range of different irradiation regimes.

Evaluation of Ablation

Upon irradiation, polymeric materials are observed to ablate by emitting their polymer component. Logically, the volume of ablated matter per pulse may be expected to depend on the amount of laser source energy E (in J/cm^3) which is actually absorbed by the material as: E = K (1-R) ε. The latter is evaluated by measuring ε and sample reflectivity R at 248nm and knowing the optical absorption coefficient K (in cm^{-1}) of the material at 248nm. Because of the limited amount of matter which is usually emitted upon one single pulse irradiation as compared to the actual surface roughness of a virgin platelet, the ablated depth per pulse Δz cannot be measured directly. Instead, one measures the total ablation depth which is obtained after a series of n successive, isoenergetic pulses and divides that depth by n (e.g. n = 20). The resulting averaged value of Δz may be moderately affected by the presence of fiber, in particular at high fluences when ablation reaches that part of the material volume with (≈ 10%) nominal fiber distribution and only after irradiating with a large enough number of pulses (n>10).

3. RESULTS

For the three materials which have been studied in this work, Δz has been measured and traced over a series of distinct irradiation experiments, each being carried out at a given measured fluence ε. Results are shown in Figs. 1 to 3, for PET, PES and PPS, respectively. Error bars refer to remanent uncertainties after smoothing experimental data. Upon increasing fluence, it is seen that i) ablation starts at a threshold fluence ε_0, and ii) z tends towards a maximum value z_0. Values for ε_0 and z_0 are quoted on figures for all three materials. As such, these quantities do not carry much physical information except for setting an apparent ablation rate for each experimented fluence.

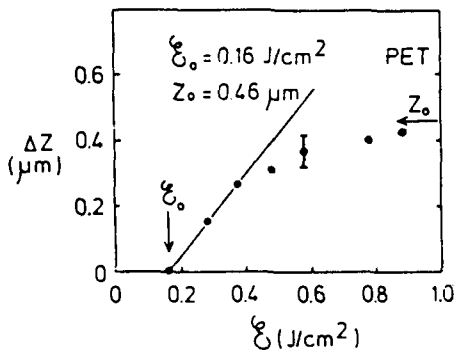

Fig.1

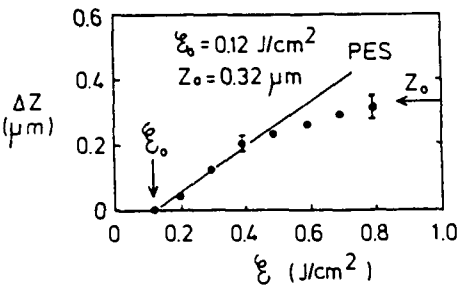

Fig.2

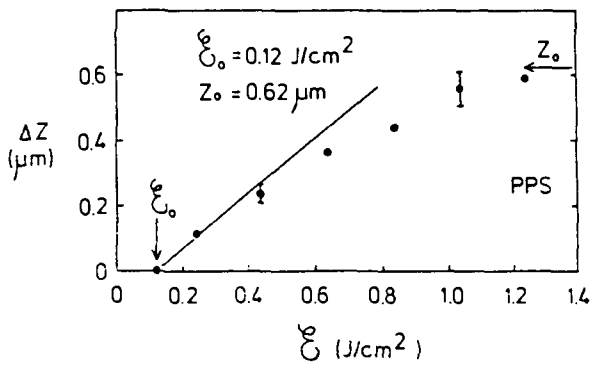

Fig.3

One may now modify the graphs of Figs. 1 to 3 by transforming:

i) the measured values of the impinging energy density (ε) into E*;

ii) those of Δz into the ratio $\Delta z / z_0 = \Delta z \times S / z_0 \times S = \Delta V / V_0 = \eta$, where S is the actual irradiated area and ΔV the ablated volume. The resulting graphs of the ablation efficiency $\eta(E^*)$ are presented in Figs. 4 to 6, together with the respective chemical configurations of the polymers, for PET, PES and PPS, respectively.

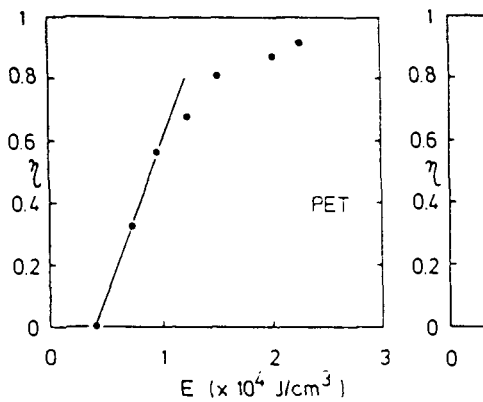

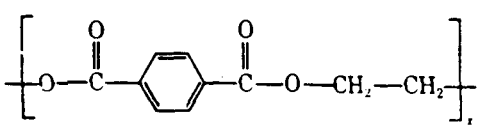

PET

Fig.4

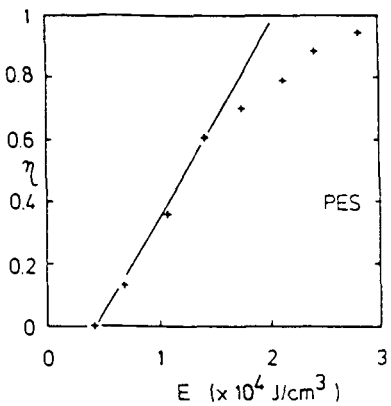

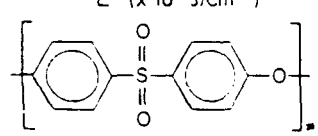

PES

Fig.5

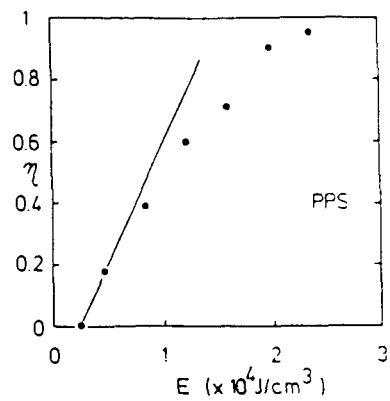

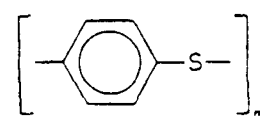

PPS

Fig.6

Two quantities are here remarkable, namely: E_0^*, or effective absorbed energy per cm^3 at ablation threshold, and χ ,the initial ablation rate at E_0^*, or $\chi = (\Delta\eta / \Delta E^*)_{E0^*}$. These quantities are given in Table 2.

The three graphs are compared in Fig.7, below. One notes that PES and PPS differ from PET with equivalent ε_0 values. In contrast, PET and PES do have close E_0^* values in sharp contrast with PPS. This is due to the lesser absorption coefficient K (and deeper light penetration, cf. Fig.3) in the latter compared to the other two materials.

The evolution of η with E* may be described via a model incorporating the above quantities. A volume v is irradiated and reduces to (v - dv) upon absorbing an energy dE. One writes a rate differential equation to describe the ablation process as:

$$-\frac{dv}{v} = \chi dE \quad \text{, where } \chi \text{ is an ablation coefficient}$$

Summation is performed as:

$$\int_{v}^{v'} -\frac{dv}{v} = \int_{E_0^*}^{E^*} \chi dE \; ; \qquad Log\frac{v'}{v} = -\chi(E^* - E_0^*) \quad \text{and} \qquad \frac{v'}{v} = \exp\left[-\chi(E^* - E_0^*)\right].$$

The ablation efficiency follows as: $\eta = \dfrac{V - V'}{V} = 1 - \exp\left[-\chi(E^* - E_0^*\right]$.

4. ANALYSIS

A few approximations and hypotheses need be introduced to understand the physical meaning of the above data:

i) the irradiation time is extremely small (40nsec) as well as the heat conductivity of the polymeric materials. Therefore, one may reasonably assume that the absorbed laser energy E (in whichever form) has no time to dissipate out of the light penetrated volume of the material (V_L) during pulse duration, i.e. all of the absorbed energy E is consumed where it has been initially deposited (i.e. no energy loss).

ii) any eventual material transformation (e.g. emission of matter) may be considered as originating solely from V_L, i.e. the maximum volume of emitted matter (V_0) is entirely contained in V_L: one makes the hypothesis that V_0 would tend to equal V_L upon increasing fluence.

iii) morphological instability in a polymeric chain stems here from exciting valence electrons via photon absorption: it should be noticed that resulting excited electrons as well as generated phonons do remain (by structure) spacially confined in each individual chain. Further, the time necessary for these excited electrons to recombine onto a valence state (setting an instability period for any corresponding atom site) is usually of the order of 5-10nsec. It is reasonable to assume that morphological instability results from the time confinement (or time overlap) of these atomic instabilities within the same chain. This would imply that no instability would result from part of the absorbed photons, in particular from those which belong to the less intense part of the emission, leaving some 50% of the absorbed laser energy (within the first 10nsec of irradiation) to be responsible for the observed ablated volume.

From these arguments, one may now proceed to interprete the above data. V_0 could be correctly approximated by evaluating the light penetration depth behind the sample irradiated area. That depth is determined by the material absorption coefficient K at any given light wavelength, irrespective of the light intensity at that wavelength. Typically and by the Lambert-De Beer definition of K, 90% of the light energy are absorbed over a light penetration length z_{90} set by the quantity $z_{90} = 2.3 / K$.The maximum ablation depth z_0 may be used to approximate z_{90} (within experimental error) as $z_{90} = 0.9\ z_0$, from which: $K = 2.55 / z_0$. All relevant values appear in Table 1.

		PET	PES	PPS
ε_0	(J/cm^2)	0.16	0.12	0.12
z_0	(μm)	0.46	0.32	0.62
z_{90}	(μm)	0.41	0.29	0.56
K	(x 10^4 cm^{-1})	5.6	7.9	4.1

Table 1

The amount of absorbed energy E per volume (in J/cm^3) is set by $E = K (1-R) \varepsilon$, where R is the material reflectivity at the laser wavelength. R is measured at: 0.07, 0.09 and 0.08 for PET, PES and PPS, respectively. Further, point iii) above is used to define an effective absorbed laser energy in terms of ablation, $E^* = 0.5\ E$.

Entering in the above equation values given in Table 2 for E_0* and η yields the graphes represented in Fig.8. A qualitative agreement is achieved with the experimental graphes, Fig.7. However, model figures for η are systematically too low for all materials compared to experimental ones (by 10% for PPS, by 15 to 20% for PES and PET). This fact may be related to uncertainties when measuring Δz in conjunction with the presence of fiber in these materials, and to light diffusion in polymeric materials.

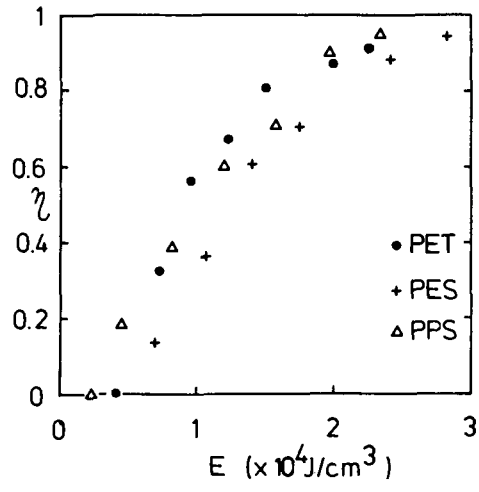

Fig.7

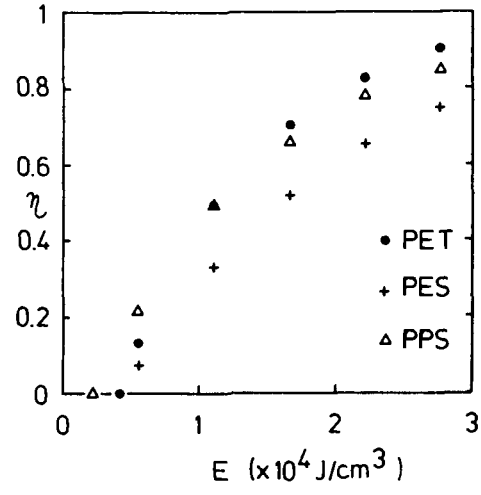

Fig.8

One may now compare the three materials through values given in Table 2. In particular, ablation threshold energies are interesting to compare with the respective monomer masses and valence electron populations, Table 2.

		PET	PES	PPS
monomer mass		192	232	108
monomer val.e⁻ number		72	74	31
E_0*	($x10^4$ J/cm³)	0.413	0.436	0.227
E_V	(eV/monomer)	14.1	16.6	4.0
α_0	(abs.phot./val.e⁻)	0.039	0.045	0.129
ΔE_V	(eV)	- 0.55	- 0.75	- 0.52
E_S	(eV)	+ 4.45	+ 4.25	+ 4.48
χ	($x10^{-4}$ cm³/J)	0.74	0.59	0.76
"	(em.at./abs.phot.)	2.37	1.89	2.44
"	(br.bond/abs.phot.)	1.18	0.94	1.22

Table 2

Clearly, the ablation threshold is proportioned to the monomer mass, thus carrying identification of a limit to tstructural stability of the polymeric chain against external sources of energy. That threshold (expressed as E_v, in eV/monomer) could reasonably

represent the internal energy of the monomer, i.e. the range of energy which is occupied by the valence electrons or valence band width. Reducing that quantity to the valence electron population times the actual photon energy (5eV) yields α_0 (expressed in absorbed 5eV photon per valence electron, Table 2) which represents, at threshold, the maximum fraction of the valence electron population, just below the top of valence band (or Fermi level, E_F) which may be effectively excited at 5eV without disturbing atom configurations, thus setting the onset of instability. That fraction α_0 may be used to determine ΔE_V, i.e. the range of electrons which contribute, at any fluence, to light absorption at 5eV: $\alpha = \Delta E_V / E_V$. The obtained values for ΔE_V (taking the energy zero at E_F) are given in Table 2. To these values, one now adds the 5eV photon energy to define a minimum level of energy E_S above E_F, at and above which valence electrons are excited over a range set by $\Delta E_C = \Delta E_V$. That level E_S is remarkably constant at 4.4 ± 0.15eV for all three polymers. It is advocated that E_S delineates most probably the surface potential of these polymeric materials and electrons excited above E_S would effectively be emitted out and permanently lost by of material. ΔE_C is set by the photon energy and may not vary with the number of 5eV photons. As a consequence, it is the actual electron population of that range (equal to the number of absorbed photons, as tuned by varying ε) which would decide for the onset of instability as materialized through atom emission (or laser ablation) at E_0*. Most remarkably, atom emission appears then to be triggered by a minimum fraction of only those valence electrons which are excited above E_S, i.e. atom emission is triggered by electron photoemission.

Once the polymer reaches destabilization and starts ablating, the initial rate of ablation χ would somehow depict the way the polymer deteriorates by emitting, at the onset of ablation, the lightest residues of the now possible monomer decomposition. It is particularly significant to notice the actual values of χ expressed in broken bonds per absorbed photon. Irrespective of the monomer, all figures obtained for these three monomers consistently amount to about one unit. These results would then support the general concept of a process which could be defined as being fully described via photoemission driven bond breaking at the irradiated material giving way to emission of matter.

Among the three polymers, PPS has by far the simplest monomer which consists of two entities: a phenyl group and a S atom which would be both liberated upon ablation. One may note that the model description (in Fig.8) is effectively very close to the experimental data (Fig.6). As experimented, S atoms eventually react to ambiant hydrogen to form characteristic H_2S molecules. In contrast, the PES monomer is far more rigid: it does not liberate free S atoms (no H_2S formed) but rather SO_2, phenyl groups and oxygen atoms. Finally, PET would be more or less equivalent to PES in terms of inner stability in relation with the size of its monomer, but would more readily decompose than PET into phenyl groups, CO_2 and weakly coupled CH_2 radicals. This potential variety of emitted particules would result in a hierarchy of specific emission regimes and rates.

5. CONCLUSION

In this work, the phenomenology of near threshold excimer induced ablation of polymeric materials has been studied. It is shown that the process reflects the inner stability of these molecular structures in setting an upper limit to their structural stability against external sources of energy. More generally, the results and their analysis reveal the intimate nature of polymer ablation to be essentially driven by intense electron photoemission.